On-Chip Hybrid Power Supply System for Wireless Sensor Nodes

Wulong Liu[1], Yu Wang[1], Wei Liu[1], Yuchun Ma[2], Yuan Xie[3], Huazhong Yang[1]
[1]Dept. of E.E., TNList, Tsinghua Univ., Beijing, China
[2]Dept. of C.S., TNList, Tsinghua Univ., Beijing, China [3]Dept. of CSE, Pennsylvania State Univ., USA
[1] Email: yu-wang@mail.tsinghua.edu.cn

Abstract—[1]With the miniaturization of electronic devices, small size but high capacity power supply system appears to be more and more important. A hybrid power source, which consists of a fuel cell (FC) and a rechargeable battery, has the advantages of long lifetime and good load following capabilities. In this paper, we propose the schematic of a hybrid power supply system, that can be integrated on a chip compatible with present CMOS process. Besides, considering the problem of maximizing the on-chip fuel cell's lifetime, we propose a modified dynamic power management (DPM) algorithm for on-chip fuel cell based hybrid power system in wireless sensor node design. Taking the wireless sensor node powered by this hybrid power system as an example, we analyze the improvement of the FC-Bat hybrid power system. The simulation results demonstrate that the on-chip FC-Bat hybrid power system can be used for wireless sensor node under different usage scenarios. Meanwhile, for an on-chip power system with $1cm^2$ area consumption, the wafer-level battery can power a typical sensor node for only about 5 months, while our on-chip hybrid power system will supply the same sensor node for 2 years steadily.

I. INTRODUCTION

In recent years, wireless sensor networks have gained increasing popularity.For example, wireless sensor networks have a great impact on environment monitoring, data collecting, danger warning etc. As we know, power is supplied with the help of energy supply system fitted with the embedded system and is not easily replaceable [1] . Thus, energy consumption has become a major challenge for embedded system design. Traditional technologies for solving energy consumption problem mainly focus on minimizing the working energy consumption of the embedded system, such as dynamic voltage scale (DVS) [2] or dynamic frequency scale (DFS) [3] , and maximizing the lifetime of the power system [4]–[6]. In this paper, we discuss how to maximize the lifetime of the power system so as to extend the lifetime of wireless sensor nodes (WSN).

In order to maximize the lifetime of power system, several energy self-supply systems have been proposed [7]. These systems could supply themselves depending on converting other energy, such as solar energy, motional energy, or chemical energy etc, to electronic energy automatically. However, these self-supply systems are not controllable, and influenced by the environment greatly. Thus, they are not good choices for the embedded system which needs power supply continuously. In this case, an external power supply system must be utilized to keep the embedded system work properly.

Meanwhile, with the miniaturization of electronic devices, the size has become one of the most important factors in WSN. For example, the size of micro-sensor has decreased to micrometer level. However, the miniaturization of sensor nodes leads to little decrease of energy consumption, sometimes the power increases indeed. On the other hand, the traditional battery with low power density and little probability to be integrated on-chip, can not be utilized to supply power for this micro embedded system.

As an alternative power source of traditional battery, fuel cell has attracted much attention. The basic characteristics of an FC are as follows [4].

1) High Energy Density: In general, compared with Li-ion battery, the fuel cell provides 4 to 10 times energy for the same size and weight.

2) Environment friendly: Typically, a FC uses hydrogen (H) and oxygen (O) to generate electrical power, and the by-products are water and heat.

3) Slow and Limited Load Following: Not similar with the traditional batteries, the fuel cells have a narrow load current following range, which is mainly caused by the fact that the slow reaction on the electrode cannot follow quick variation of the load current.

Therefore, fuel cell alone can not meet the power demands of an embedded system with large and frequent current fluctuations. Consequently, one practical solution, hybrid power system, has been proposed [4]–[6]. A typical hybrid power system consists of fuel cells worked as the primary source and a rechargeable battery or a supercapacitor worked as the secondary source. In this hybrid power source, the rechargeable battery or the supercapacitor stores surplus energy from the fuel cell during the low demand periods, and provides excessive current during the peak load current demand period. For the reason that the supercapacitor has lower energy density than the battery, and output voltage of the supercapacitor varies with its charge capacity [8], in our work, the hybrid power system is made up of fuel cells and rechargeable battery.

From the above discussion, power supply system with small size and high energy density has been one of the most important factors in embedded system design. In this paper, we present a hybrid power system for wireless sensor nodes design. Our contributions includes:

1) We explore the possibility of an on-chip fuel cell based hybrid power system for embedded systems, especially for the wireless sensor nodes design. Since the development of the three-dimensional (3D) integration provides a new chance for integrating different processes on one chip, we also discuss the integration method of the hybrid power system and the sensor circuity.

2) We proposed a dynamic power management algorithm realized by regulating the fuel cell current to minimize the energy consumption and extend the lifetime of wireless sensor nodes.

The rest of the paper is organized as follows. Section II describes the previous work related with our research. Section III introduces the schematic of the hybrid power system and discuss the possible 3D integration with sensor circuit. We then describe the detailed modeling of this hybrid power system for WSN in Section IV. Section V presents the simulation method and discusses the simulation results. Finally, we conclude the paper in Section VI.

II. RELATED WORK

A. Hybrid Power Systems

Many hybrid power system structures have been proposed. In general, they can be divided into four categories depending on their components: fuel cell-battery hybrid power system [4]–[6], fuel cell-supercapacitor hybrid power system [8]–[13], battery- supercapacitor hybrid power system [14]–[16], and fuel cell-supercapacitor-battery hybrid power system [17]–[19]. Fuel cell-battery hybrid power system combining the characteristics of fuel cell's high energy density and battery's good load current following ability has been widely used in some portable devices, such as camcorders. With the characteristics of fuel cell's high energy density, supercapacitor's high capacity and quick charging or discharging ability, but no transitory step current provided, fuel cell-supercapacitor hybrid power system is always utilized to power some high power devices, such as the vehicles. For battery-supercapacitor hybrid power system, which has relative low energy density comparing with fuel cell-supercapacitor hybrid power system, is always utilized as energy storage system for wind applications or power supply system for some vehicles. Fuel cell-battery -supercapacitor hybrid power system has high energy density, long cycle life, good load current following ability, and etc. However, these advantages are achieved at the cost of large area. In summary, supplying power for some low power devices, especially on-chip devices, such as micro sensor node, **fuel cell-battery hybrid power system is the best choice**.

B. Fuel Cell integration and Power Management

Besides, a numerous work has been done focused on 2D fuel cell miniaturization and integration so that we can achieve higher power density with smaller footprint. Frank et al. [20], [21] proposed a new integrated power supply system using on-chip polymer electrolyte membrane (PEM) fuel cells. This power supply system is managed by some CMOS circuits control units, and it can be realized within an extended CMOS process. The detailed fabricated processes and the characteristics of on-chip fuel cells were presented in [21]. Notten et al. [22] described a 3D-integrated all-solid-state battery concept, which could prevent electrode degradation upon cycling and electrolyte leakage.

As we mentioned before, the power management of hybrid power system is critical for the system lifetime. Zhuo et al [4]–[6] proposed dynamic power management algorithm to maximize the lifetime of some "big" embedded systems, such as camcorders. Because of its limitation on miniaturization, this system is not suitable for some "small" systems, such as on-chip wireless sensor nodes. Therefore, in the paper, we propose the schematic of on-chip fuel cell based hybrid power system which can be compatible with CMOS process. What's more, we propose a modified dynamic power management method for the wireless sensor node.

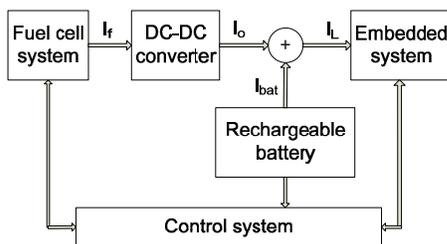## III. HYBRID POWER SYSTEM FOR WIRELESS SENSOR NODE

Fig. 1.   The schematic of the hybrid power system for wireless sensor node.

A. The Schematic of Hybrid Power System

The schematic of the hybrid power system is shown in Figure 1. This hybrid power system consists of fuel cells, rechargeable batteries, DC-DC converter, and control unit. When the fuel cell current I_o is larger than the load current I_L, external power energy will be used to recharge the battery. Once the battery is full of charge, the external power energy will be bypassed to ground. When the fuel cell current I_o is less than the load current I_L, the rechargeable battery will provide the current difference $I_L - I_o$. In this way, we use a dynamic power management algorithm in the control system to minimize the fuel consumption.

B. Components of the Hybrid Power System

1) on-chip Fuel Cell: Conventional PEM fuel cells consist of a polymer electrolyte membrane (PEM), two gas diffusion electrodes, two diffusion layers, and two flow fields. The reactants, e.g. hydrogen and oxygen, are supplied to the gas diffusion electrodes over feed pipes out of external tanks. The amount of supplied fuel is often controlled by active system periphery like pressure reducers and valves.
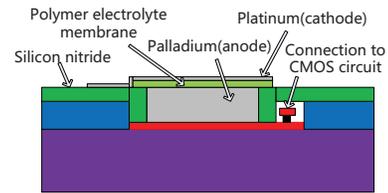

Fig. 2.   Structure of a chip integrated fuel cell.

For a chip integration PEM fuel cell [21], it is made up of a palladium based hydrogen storage and an air breathing cathode both separated by a PEM. Similar with the conventional fuel cell, the FC uses H_2 and O_2 to convert chemical energy to electricity by an electro-chemical process. The hydrogen (H) atoms stored within the palladium are split up into protons and electrons. The electrons flow through the external circuit to the cathode and drive the load. The protons are transported to the cathode through the proton conductive PEM. At the cathode, electrons, protons, and oxygen - supplied by the ambient air - catalytically recombine to water [20], [23]. Comparing with conventional FC, chip integration PEM fuel cell does not need external fuel storage and transporting devices. Thus, it can be realized within extended CMOS process. The structure of an integrated fuel cell is illustrated in Figure 2. Actually, the chip integrated fuel cell has the capacity of $500mAh/cm^2$. Compared with state-of-the-art wafer level batteries, $45mAh/cm^2$, the fuel cell has the potential to provide much more capacity [21].
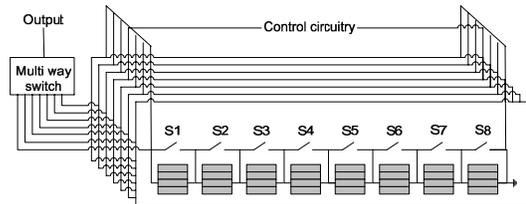

Fig. 3.   On-chip fuel cell cascades modeling in our hybrid power system.

The whole fuel cells connection is shown in Figure 3. The system consists of some fuel cell cascades (FCCs) connected in parallel. Every fuel cell cascade is made up of 8 fuel cells, which will provide 3V open voltage. Besides, we use an external multi-way switch to control output current of the FCCs by controlling the connected

number of FCCs. According to the control signal, we select several FCCs to output current in turn, which will avoid unfair usage of the FCCs and extend the fuel cell lifetime.

2) On-Chip Rechargeable Battery: Thin film Si-intercalation electrodes covered with a solid-state electrolyte are found to prevent electrode degradation upon cycling and electrolyte leakage, and has a high energy density appropriately $5mWh/um * cm^2$. Besides, comparing to a super capacitor, the rechargeable batteries have an appropriately constant output voltage. What's more, their energy capacity is more than 3 orders of magnitude higher than that of integrated capacitors. The model of 3D integrated all-solid-state Li-ion battery is shown in Figure 4.
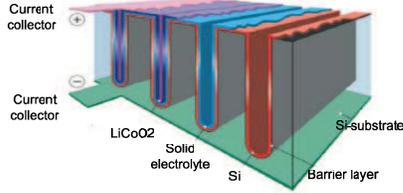

Fig. 4. All solid state Li-ion battery that can be integrated into the 3D hybrid power system [22].

3) Power Control Unit and the Embedded System: In this work, we use the wireless sensor node to act as the embedded system powered by the hybrid power system. Besides, in the whole system, only one processing unit is used, which will handle the data of wireless sensor node and manage the hybrid power system.

C. Hybrid Power System Allocation

In order to improve the form factor and consider the cost at the same time, the hybrid power system and sensor circuity can be integrated in one chip or separatedly allocated on the PCB board. The separated allocation of the power system and sensor circuity will consume larger space with lower cost, while the fully integrated one (e.g. 3D integration with system in a package) will have relatively higher cost but smaller footprint. Here we only discuss the possible 3D integration case shown in Figure 5:
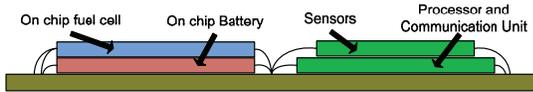

Fig. 5. Structure of the Hybrid Power System for Wireless Sensor Node.

1) The on-chip hybrid power system: Considering the working principle of the fuel cell, the cathode needs to breathe the oxygen from the surrounding air, so we put the fuel cell on the top layer. As shown in Figure 2, first of all, worked as the interconnection line, a thin polysilicon film is grown on the p-sub. Then, about 5um palladium related with H atoms is deposited on the polysilicon. Next, 5-10um PEM is deposited by CVD technology. Finally, about 200nm platinum is sputtered on the PEM worked as the anode material [21].

To reduce the energy consumption caused by the parasitic effect, the rechargeable batteries will be placed on the second layer.

2) 3D structure of wireless sensor node: The sensor node structure mainly consists of three parts: Data Sensing unit, Processing unit, and Data Communication unit. The date sensing unit is put on the top level, and the processing unit and data communication unit are placed on the bottom level.

IV. MODELING AND POWER MANAGEMENT FOR HYBRID POWER SYSTEM

A. Fuel Cell Modeling

According to the actual I-V characteristic of the FCCs, we divide it to three regions: the activation region, ohmic region, and concentration region [24].

1) Activation Region: A diode can be utilized to simulate the behavior of the activation region: $V_A = Aln(I_f/I_n)$, in which I_n represents the current when I-V characteristic turns from the activation region to ohmic region, I_f is the output current of fuel cells and A is a coefficient.

2) Ohmic Region: One simple resistance could be used to model the ohmic region: $V_R = RI_f$, in which R is a coefficient.

3) Concentration Region: A transistor can be used to simulate the concentration region: $V_c = mI_me^{nI_mI_f}$, in which m, n are coefficients, I_m represents the current when I-V characteristic turns from the ohmic region to concentration region.

The mathematical I-V characteristic of FC is modeled as $V = E - Aln(I_f/I_n) - RI_f - mI_me^{nI_mI_f}$, in which E is the ideal open voltage of FC. Table I and Figure 6 show the fuel cells' model parameters, I-V characteristics and power plot of fuel cells respectively. Fuel cells have the maximum output power worked at appropriate 1V output voltage which is point out in Figure 6.

TABLE I
PARAMETERS USED IN OUR FC MODELING.

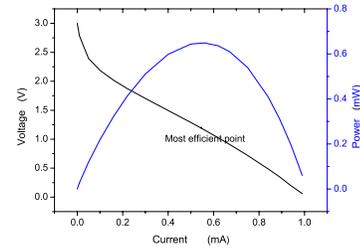| Parameters	E (V)	A	I_n (A)	R (Ω)	m	n	I_m (A)
Value	3	0.5	0.3	0.007	1.35	1.5	0.7

Fig. 6. Polarization and power plot of FCCs. The most efficient point represents the maximum power point.

B. Rechargeable Battery Modeling

According to the measured data presented in [22], the model of on-chip battery is similar to the characteristic of traditional Li-ion rechargeable batteries as the following expressions.

$$V = \begin{array}{l} 0.5 * SOC + 0.8, 0 < SOC \leq 0.2 \\ 0.25 * SOC + 0.85, 0.2 \leq SOC < 1 \end{array} \quad (1)$$

and

$$SOC = (\int_0^t (I_o - I_l)dt)/C_{max} \quad (2)$$

where SOC is the state of charge, I_l is the load current, I_o is the output current, C_{max} is is the maximum capacity of rechargeable battery.

C. DC-DC Converter Modeling

Since the output voltage of fuel cell and rechargeable battery tends to be a constant, we define the FCCs and DC-DC converter system's converting efficiency using a linear model [5] as $\eta = \alpha - \beta I_o$, where α, β are the empirical value decided by the actual converting efficiency.

D. Dynamic power management algorithm

TABLE II
DEFINITIONS IN OUR DYNAMIC POWER MANAGEMENT ALGORITHM FOR WSN

C_{max}	The maximum charge capacity of the battery
I_{max}	The maximum output current of the fuel cell
I_{min}	The minimum output current of the fuel cell
$Q_{ini}(k)$	The charge state of the battery at the initial of Kth task
$Q_{end}(k)$	The charge state of the battery at the end of Kth task
$I_{o|s}(k)$	The output current of the DC-DC converter at the Sleep state
$I_{o|A}(k)$	The output current of the DC-DC converter at the Active state
$I_{l|S}(k)$	The load current at the Sleep state
$I_{l|lis}(k)$	The load current at the Listening state
$I_{l|C}(k)$	The load current at the Communication state
$T_S(k)$	The Sleep state time
$T_I(k)$	The Idle state time
$T_{lis}(k)$	The Listening state time
$T_C(k)$	The Communication state time
I_{fc}	The output current of the fuel cell
μ_{sp}	The permitted maximum idle time
μ_a	The permitted time to regulate the fuel cell current in Active period

Based on the dynamic power management algorithm on hybrid power system [5], we propose a hybrid power system optimization method for wireless sensor node. The wireless sensor node has four states: *Sleep*, *Idle*, *Listening*, and *Communication*. Firstly, once $T_I(k) > \mu_{sp}$, the power system will be put into *Sleep* state. We consolidate the *Listening* and *Communication* states as Active state. Then, in the *Sleep* state, the battery will be charged. In the *Active* state, the battery will be discharged to provide the external load current. As we know, the *Communication* state needs a large current and the battery has a well load current following ability. Thus, when the fuel cell current tends to be constant during the *Active* state, the battery could provide this peak current rapidly. Because the output voltage of fuel cells can be regulated by DC-DC converter at an approximate constant. And the input or output voltage of battery has little variation, thus, in this work, we just consider the current for simplification. The outline of our modified dynamic power management algorithm is shown in Figure 7.

We begin with some definitions used in this algorithm as shown in Table II. Our goal is to minimize the fuel consumption for each task. We assume that $I_{o|A}(k)$, $I_{o|s}(k)$ are constants during the k-th task slot. $T_s(k)$, $T_{lis}(k)$, $T_C(k)$ could be obtained from the load profile before we perform the task. Besides, according to the DC-DC converting efficiency,

$$I_{fc} = (V_o \times I_o)/(\xi \times \eta) \approx (0.3 \times I_o)/(\alpha - \beta I_o) \quad (3)$$

where V_o is the output voltage of DC-DC converter, and ξ is the power efficiency of fuel cell.

Hence, the fuel consumption is given by

$$C(k) = (0.3 \times I_{o|s}(k))/(\alpha - \beta I_{o|s}(k)) + \quad (4)$$
$$(0.3 \times I_{o|A}(k) \times (T_{lis}(k) + T_C(k)))/(\alpha - \beta I_{o|A}(k))$$

Then taking the battery state for consideration, in each k-th task slot, we consider the case when $Q_{ini}(k) \neq Q_{end}(k)$. Since

$Q_{ini}(k) = Q_{end}(k-1)$, $Q_{ini}(k)$ is a known value. We suppose that $Q_{end}(k) = Q_{ini}(1)$ for each round optimization. According to the rule of conservation of charge, we give out the following expression.

$$Q_{ini}(k) + (I_{o|s}(k) - I_{l|s}(k)) \times T_s(k) = \quad (5)$$
$$(I_{o|lis}(k) - I_{o|A}(k)) \times T_{lis}(k) + (I_{o|c}(k) - I_{o|A}(k)) \times T_C(k)$$
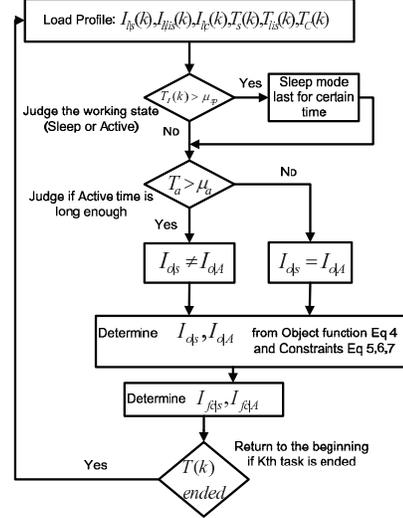

Fig. 7.   Our modified DFM algorithm for WSN.

Besides, in each cycle, we define that the ending discharge state pluses the discharging capacity should be less than the maximum capacity of the battery, which can be indicated by the following expression.

$$Q_{end}(k) + (I_{l|lis}(k) - I_{o|A}(k)) \times T_{lis}(k) +$$
$$(I_{l|c}(k) - I_{o|A}(k)) \times T_C(k) \leq C_{max} \quad (6)$$

Then, because of the narrow load current range of the fuel cells, we define the limitation that

$$I_o \in [0.01, 1] \quad (7)$$

Thus, when expression (4) is taken as the **objective function** and expressions (5), (6), (7) as the **constraints**, we can find out the optimal value of $I_{o|s}(k)$ and $I_{o|A}(k)$. At last, the output current of fuel cell I_{fc} during *Active* and *Sleep* modes can be decided by expression (3).

We also consider two extreme operation cases. First, if active time $T_a = T_{lis}(k) + T_C(k) \leq \mu_a$ in one task, that means the active time is too short, we will keep the output current of the fuel cell as constant: $I_{o|s}(k) = I_{o|A}(k) = I_o(k)$. In the other case, if active time or communication time $T_C(k)$ in one task lasts too long and cannot meet constraints in equation (5) and (6). We define that both the initial charge of battery in k-th task and the charging capacity during *Sleep* period equal to the discharging capacity in listening period which can be expressed in equation (8). While during the *Communication* state, all the current demand will be only provided by regulating the multi ways switch in FCCs, which means to increase the output current of FCCs, although the FCCs' efficiency will be lower. Therefore equation (8) will take place of equation (5) as a constraint.

$$Q_{ini}(k) + (I_{o|s}(k) - I_{l|s}(k)) \times T_s(k) =$$
$$Q_{end}k + (I_{l|lis}(k) - I_{o|A}(k)) \times T_{lis}(k) \qquad (8)$$

V. Experimental Results

A typical wireless sensor node applied in low duty cycle is utilized in our work, which mainly consists of Micaz and MTS310 [25], and has a 7.3728MHZ working frequency, 250 kbps transferring rate. Two types of data, Light and Temperature information, are acquired in each cycle (the cycle time is 70 seconds). This acquired information could be transferred in its cycle or accumulated into another cycle to be transferred together. In Figure 8, the current consumption within one working cycle is presented and scaling to on-chip integrated conditions. In this work, from the point of minimized energy consumption, we will evaluate how the hybrid power system behaves and then find out the most efficient operating pattern.
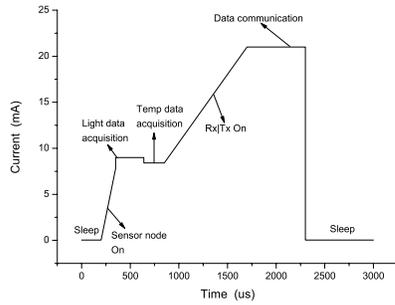

Fig. 8. A typical current load profile of a wireless sensor node.

Figure 9 shows the simulator in Matlab/Simulink used in our experiment. First of all, we compare this on-chip FC-Bat hybrid power system with traditional wafer-level battery as shown in Table III. When the chip area is assumed as $1cm^2$ and the whole power system has two layers, the wafer-level battery's capacity is about 45*2=90mAh, while on-chip FC-Bat hybrid power system's capacity is 500mAh [21]. The simulation results demonstrate that the wafer-level battery can power a typical sensor node for only about 5 months, while our on-chip hybrid power system could supply a typical sensor node for over 2 years steadily.
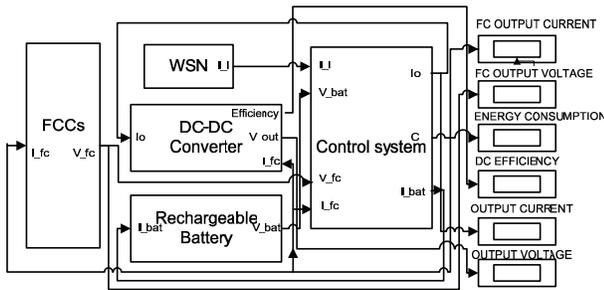

Fig. 9. FC-Bat hybrid system simulator in Matlab/simulink.

By regulating sensor node's operated cycle numbers of data acquisition, we obtain the total and average energy consumption in five operation modes as shown in Table IV. Comparing with the situation

TABLE III
COMPARISON OF TWO KINDS OF POWER SOURCES. EC: ENERGY CONSUMPTION

Power Source	Chip Area cm^2	Capacity (mAh)	EC per cycle (mJ)	Life time (year)
Wafer-level battery [26]	1	45*2	1.9208	0.374
Hybrid power system	1	500	1.614	2.475

TABLE IV
ENERGY CONSUMPTION (EC) OF FIVE WORKING PATTERNS (mJ).

Operation modes: Communication within	Total EC	Average EC per cycle	EC with battery only
one cycle	1.6140	1.6140	1.9208
two cycles	3.214	1.6070	3.8292
three cycles	4.8152	1.6051	5.7375
four cycles	6.4173	1.6043	7.6459
five cycles	8.0184	1.6037	9.5542

that powered with only wafer-level battery, our proposed DPM algorithm on FC-Battery hybrid power system can save 16% more energy. From Figure 8, the sensor node gets light and temperature data in each cycle, but we can save them and transfer the data at one time. From Table IV, we conclude that the more acquisition data stored to be transferred in one cycle, the less energy will be consumed by one sensor node per cycle. However, from the curve of average energy consumption per cycle with five operation modes showed in Figure 10, we find that the average energy consumption per cycle will reduce little after the communication period is greater than 4 cycles. Meanwhile, the stored acquisition data numbers are directly proportional to the efficiency of data storage and processing. Comprehensively considered, the operation mode with four acquisition cycles and data transferred in the fourth cycles will be the most efficient operation mode in our scenario.
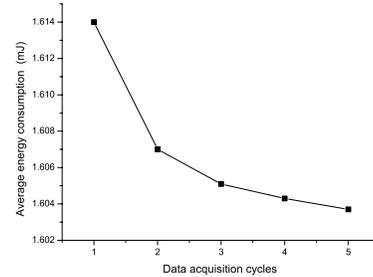

Fig. 10. Average energy consumption per cycle with five operation modes.

Figure 11 gives the detailed FCCs output current I_o during data communication cycle in six operation modes (transferring 0-6 data packages). We can see from the current profile, I_o variation located among the region of $[0, 1mA]$. Because larger variation of I_{fc} between active and sleep states results in larger fuel consumption, the output current under DPM algorithm is much more flatter and results in lower fuel consumption according to Equation (3).

We keep all the conditions the same of a typical data transferred within one cycle but regulating the Sleep state's time. This corresponds to the curve shown in Figure 12. The results show that energy consumption in one operation cycle increases in linear relation with the cycle time. Besides, holding the cycle time as 70s, when we change the communication/active time, the relation of active time, energy consumption, and transferred data is shown in Figure 13, which demonstrates that energy consumption in data communication cycle is proportional to the amount of communicated data.

Then, we discuss one case that one task is accomplished in a 70s working cycle and another case that one task is accomplished within five subtasks which has a 14s cycle time. The simulation results in Table V show that one task accomplished within five cycles has less energy consumption than one task accomplished in one cycle.

Finally, we consider two extreme working states of sensor node as shown in Table VI. The simulation results demonstrate that when the sensor node works at the extreme states, FC-Bat hybrid power system also has less energy consumption than the one powered with battery only.
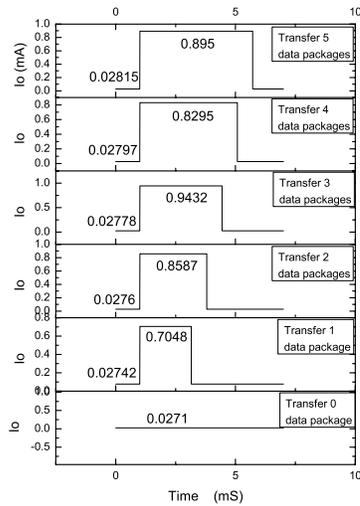
Fig. 11. Output Current of fuel cell within one transferring cycle in six working states.
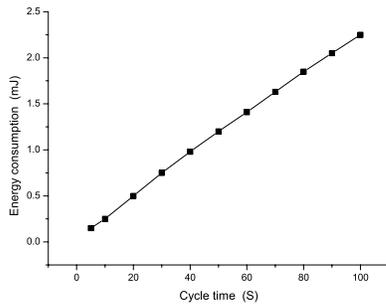

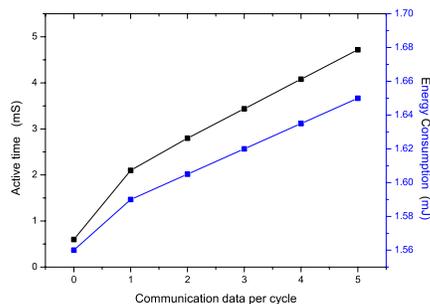Fig. 12. Energy consumption per cycle varies with the cycle time.

Fig. 13. Active time and energy consumption under six communication modes.

TABLE V
SIMULATION RESULTS IN ONE WHOLE TASK OR FIVE SUB-TASKS. I_{o-a} AND I_{o-i} ARE THE OUTPUT CURRENT FOR ACTIVE STATE AND IDLE STATE.

Operation mode	I_{o-a} (mA)	I_{o-i} (mA)	Battery capacity (mAs)	Energy Consumption (mJ)
One Task	0.996	0.03646	0.70	2.6470
Five subtasks	0.998	0.03623	0.14	2.6145

TABLE VI
SIMULATION RESULTS OF TWO EXTREME OPERATION STATES. TIME IN s, ENERGY CONSUMPTION (EC) IN mJ

Operation state	Active time	Cycle time	Hybrid EC	Battery only EC
Long active state	0.1	70	3.6857	4.0016
Short active state	0.001	70	1.588	1.9043

VI. CONCLUSIONS

In this paper, we proposed the schematic of fuel cell based on-chip FC-Bat hybrid power system which consists of on-chip fuel cells served as the primary source and on-chip rechargeable battery served as the secondary source. Then, we addressed the problem of maximizing the lifetime of a fuel-cell based hybrid power system. We proposed an power control method based on traditional dynamic power management for on-chip FC-Bat hybrid power system used in WSN. Taking the wireless sensor node powered by this hybrid power system as an example, the simulation results demonstrated that compared with wafer-level battery, FC-Bat hybrid power system can achieve about 16% energy saving. For one on-chip power system with $1cm^2$ area, the wafer-level battery can power a typical sensor node for only about 5 months, while our on-chip hybrid power system can supply the same sensor node for over 2 years steadily.

REFERENCES

[1] Y. Pal, L. Awasthi, and A. Singh, "Maximize the lifetime of object tracking sensor network with node-to-node activation scheme," *IEEE on IACC*, pp. 1200–1205, 2009.
[2] L. Yuan and G. Qu, "Analysis of energy reduction on dynamic voltage scaling-enabled systems," *IEEE Trans on CAD*, vol. 24, pp. 1827–1837, Dec. 2005.
[3] Z. Yuhua and Q. Longhua, "A dynamic frequency scaling solution to dpm in embedded linux systems," *IEEE trans on Information Reuse & Integration*, pp. 256–261, 2009.
[4] J. Zhuo and C. Chakrabarti, "Maximizing the lifetime of embedded systems powered by fuel cell-battery hybrids," *IEEE Trans. VLSI Syst*, vol. 17, pp. 22–32, 2009.
[5] K. Lee, N. Chang, and J. Zhuo, "A fuel-cell-battery hybrid for portable embedded systems," *ACM Trans on Computational Logic*, vol. 1, pp. 1–34, 2008.
[6] J. Zhuo, C. Chakrabarti, N. Chang, and S. Vrudhula, "Extending the lifetime of fuel cell based hybrid systems," *DAC 2006 43rd ACM/IEEE*, pp. 562–567, 2006.
[7] S. Benecke, N. Nissen, and H. Reichl, "Environmental comparison of energy scavenging technologies for self-sufficient micro system applications," *IEEE on ISSST*, pp. 1–6, 2009.
[8] W. Gao, "Performance comparison of a fuel cell-battery hybrid powertrain and a fuel cell-ultracapacitor hybrid powertrain," *IEEE Trans. Vehicular Technology*, vol. 5, pp. 846–855, May 2005.
[9] L. P. Boulon, "Energetic macroscopic representation of a fuel cell-supercapacitor system," *IEEE VPPC*, pp. 290–297, 2007.
[10] F. B. Ciancetta, "System pem fuel cell-supercapacitor: Analysis in transitory conditions," *ICCEP*, pp. 154–158, 2009.
[11] B. V. Capponi, "A fuel cell-supercapacitor power supply for portable applications," *COMPEL*, pp. 1–4, 2008.
[12] A. P. Payman, "Flatness based control of a fuel cell-supercapacitor multi source/multi load hybrid system," *EPE 09. 13th European conf. Power Electronics and Applications*, pp. 1–10, 2009.
[13] Z. Z. Thomsen, "A two-stage dc-dc converter for the fuel cell-supercapacitor hybrid system," *ECCE*, pp. 1425–1431, 2009.
[14] W. Li and J. G, "A power electronic interface for a battery supercapacitor hybrid energy storage system for wind applications," *PESC, IEEE*, pp. 1762–1768, 2008.
[15] Y. Zhang and etc, "Small-signal modeling and analysis of battery-supercapacitor hybrid energy storage systems," *PES 09, IEEE*, pp. 1–8, 2009.
[16] S. Pay and Y. Baghzouz, "Effectiveness of battery- supercapacitor combination in electric vehicles," *PTC 2003, IEEE*, vol. 3.
[17] F. Ciancetta and etc, "The modeling of a pem fuel cell-supercapacitor-battery system in dynamic conditions," *PTC. 2009. IEEE*, pp. 1–5.
[18] P. Thounthong and etc, "Control of fuel cell/ supercapacitor hybrid source for vehicle applications," *ICIT. 2009. IEEE*, pp. 1–6.
[19] P. Thounthong and etc., "Performance evaluation of fuel cell/battery/supercapacitor hybrid power source for vehicle applications," *IAS. 2009. IEEE*, pp. 1–8.
[20] M. Frank, M. Kuhl, G. Erdler, and I. Freund, "An integrated power supply system for low-power 3.3v electronics using on-chip polymer electrolyte membrane (pem) fuel cells," *ISSCC Dig. Tech.*, pp. 292–293, 2009.
[21] ——, "An integrated power supply system for low-power 3.3v electronics using on-chip polymer electrolyte membrane (pem) fuel cells," *IEEE Journal of Solid-State Circuits*, vol. 45, pp. 205–213, 2010.
[22] P. H. Notten, F. Roozeboom, and R. A. Niessen, "3-d integrated all-solid-state rechargeable batteries," *Adv. Mater*, vol. 19, p. 4564C4567, 2007.
[23] G. Erdler and M. Frank, "Chip integrated fuel cell," *19th European Conference on Solid-State Transducers*, vol. 132, pp. 331–336, 2006.
[24] G. L. Arsov, "Improved parametric pspice model of a pem fuel cell," *IEEE OPTIM 2008. 11th. Conference*, pp. 203–208, 2008.
[25] M. Kramer and A. Geraldy, "Energy measurements for micaz node," *Technical Report*, 2006.
[26] J. Song and et al., "Solid-state microscale lithium batteries prepared with micro-fabrication processes," *J. Micromech. Microeng*, vol. 19, 2009.